2012

Structural properties and magnetic phase transition in HoNi2Mn (57Fe)

J L. Wang
University of Wollongong, jianli@uow.edu.au

Stewart J. Campbell
University Of New South Wales,University Of New South Wales, stewart.campbell@adfa.edu.au

M Hofmann
Technical University Of Munich

M Hoelzel
Technical University Of Munich,Technical University Darmstadt

Rong Zeng
University of Wollongong, rzeng@uow.edu.au

See next page for additional authors

Authors

J L. Wang, Stewart J. Campbell, M Hofmann, M Hoelzel, Rong Zeng, S. X. Dou, and S J. Kennedy

Structural properties and magnetic phase transition in HoNi2Mn (57Fe)

J. L. Wang, S. J. Campbell, M. Hofmann, M. Hoelzel, R. Zeng et al.

Related Articles

Additional information on J. Appl. Phys.

Structural properties and magnetic phase transition in HoNi$_2$Mn (^{57}Fe)

J. L. Wang,[1,2,3,a)] S. J. Campbell,[3] M. Hofmann,[4] M. Hoelzel,[4,5] R. Zeng,[1] S. X. Dou,[1] and S. J. Kennedy[2]

[1]*Institute for Superconductivity and Electronic Materials, University of Wollongong, Australia*
[2]*Bragg Institute, ANSTO, Lucas Heights, NSW 2234, Australia*
[3]*School of Physical, Environmental and Mathematical Sciences, The University of New South Wales, Canberra ACT 2600, Australia*
[4]*Forschungsneutronenquelle Heinz Maier-Leibnitz (FRM II), Technische Universität München, Germany*
[5]*Fachbereich Materialwissenschaften, Technische Universität Darmstadt, 64287 Darmstadt, Germany*

The structural and magnetic properties of HoNi$_2$Mn(^{57}Fe) have been investigated. The ^{57}Fe-doped HoNi$_2$Mn compound crystallizes in the MgCu$_2$-type structure with *Fd-3m* space group similar to HoNi$_2$ and HoMn$_2$. HoNi$_2$Mn(^{57}Fe) exhibits ferrimagnetic ordering below a Curie temperature of $T_C \sim 60$ K—significantly higher than the corresponding values for HoNi$_2$ ($T_C = 15$ K) and HoMn$_2$ ($T_C = 24$ K)—with analyses of dc magnetization and ac susceptibility results confirming that the magnetic transition at T_C is second order. The Mössbauer spectra above T_C are described well by two sub-spectra representing the 8*a* and 16*d* sites while below T_C the spectra have been fitted using a site model comprising three sub-spectra. The Debye temperature, $\theta_D = 190(20)$ K, has been determined. © *2012 American Institute of Physics*. [doi:10.1063/1.3677666]

INTRODUCTION

Intermetallic compounds of composition AB_2 have high symmetry and are topologically closed-packed structures.[1] Their simple crystal structure and excellent physical properties make them potentially suitable for industrial and technology applications such as hydrogen storage material,[2] superconductor,[3] and giant magnetostrictive material.[4] The AB_2-type compounds have three kinds of structures: cubic C15 (MgCu$_2$), hexagonal C14 (MgZn$_2$), and dihexagonal C36 (MgNi$_2$).[1] Quite recently, it was found that one series of RNi$_2$Mn alloys with $R =$ Tb, Dy, Ho, and Er can also form the MgCu$_2$-type structure even though the ratio of rare-earth to transition-metal atoms is 1:3. These RNi$_2$Mn alloys are found to be isostructural to RNi$_2$ and RMn$_2$ compounds but with much higher magnetic ordering temperatures.[5–7]

As part of our systematic investigation[8,9] of the magnetic properties of this RNi$_2$Mn system, here we present a detailed investigation of the critical magnetic properties of HoNi$_2$Mn(^{57}Fe).

EXPERIMENTAL PROCEDURES

The HoNi$_2$Mn(^{57}Fe) sample (doped with 0.5 wt. % ^{57}Fe) was prepared by standard argon arc-melting. The sample was characterized by x-ray diffraction (CuKα radiation; $\lambda = 1.5418$ Å). Alternating current magnetic ac susceptibility and dc magnetization measurements were carried out using a conventional physical properties measurement system (PPMS-9). The powder neutron diffraction patterns were collected on the Wombat diffractometer ($\lambda = 2.4173$ Å; OPAL, Australia) at $T = 300$ K and the SPODI diffractometer ($\lambda = 1.5487$ Å; FRM II, Germany) at $T = 3$ K

and 50 K. The ^{57}Fe Mössbauer spectra were obtained over 5–300 K using a standard constant-acceleration spectrometer and a ^{57}CoRh source.

RESULTS AND DISCUSSION

Figure 1 shows the temperature dependence of the magnetization measured on the powder sample of HoNi$_2$Mn(^{57}Fe) in an applied magnetic field of 5 mT. The sample was measured on warming after first cooling in zero field (marked as ZFC). The field-cooled cooling magnetization curve, FCC, was then recorded on cooling from 300 K to 5 K. It can be seen from Fig. 1 that different thermo-magnetic behavior is detected for the ZFC and FCC magnetization curves below 46 K. This behavior can be ascribed to the magnetohistory effect originating from the narrow magnetic domain pinning.[10] The presence of narrow walls requires a large ratio of the anisotropy energy to the exchange energy[10] and it has been reported[11] that the exchange interactions are weak compared with the crystal-field effects (anisotropy) in HoNi$_2$. Based on the similarity of HoNi$_2$ and HoNi$_2$Mn (similar crystal structure and related low T_C), the necessary conditions for the presence of narrow magnetic domain pinning can be satisfied in HoNi$_2$Mn systems. The propagation of these narrow walls needs thermal activation[10] and the required energy becomes available when the temperature is increased from 5 K. Similar behaviors have been observed for other RNi$_2$Mn compounds.[5,8,9] The transition temperature has been determined from M^2-versus-T plots to be $T_C = 60$ K; this transition is significantly higher than those of the corresponding HoNi$_2$ ($T_C = 15$ K)[12] and HoMn$_2$ ($T_C = 24$ K)[13] compounds, but slightly lower than that reported for pure HoNi$_2$Mn ($T_C = 75$ K).[5] As is evident from the inset to Fig. 1, above T_C the inverse susceptibility ($\mu_0 H/M$) of HoNi$_2$Mn follows Curie-Weiss behavior leading to a paramagnetic Weiss
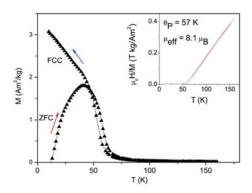
a)Electronic mail: jianli@uow.edu.au.

FIG. 1. (Color online) Temperature dependence of the dc magnetization of $HoNi_2Mn(^{57}Fe)$ measured in an applied field of ($\mu_0H = 5$ mT) under ZFC and FCC conditions. The inset shows the temperature dependence of the inverse susceptibility (μ_0H/M).

FIG. 3. Temperature dependence of the ac magnetic susceptibility of as measured in the dc magnetic fields indicated: $\mu_0H_{dc} = 2$ T to 8 T at a step of 1 T with $f = 1000$ Hz and $\mu_0H_{ac} = 0.001$ T.

temperature $\theta_p = 57$ K, and an effective magnetic moment of $\mu_{eff} = 8.1 \mu_B$.

Typical M-versus-μ_0H curves are shown in Fig. 2(a) for the magnetic region of interest (10–60 K) with the corresponding Arrott plots of M^2 versus μ_0H/M shown in Fig. 2(b). The positive slopes in the isothermal Arrott plots indicate that the transition at T_C is second order. The response of the magnetic ac susceptibility to an increasing dc field (Fig. 3) reveals several interesting features: (i) a series of critical susceptibility maxima χ_m, (ii) a decrease in the magnitude of χ_m, and (iii) a shift in the χ_m temperature to higher temperatures. As discussed elsewhere,[14] these maxima are a characteristic signature of a second-order paramagnetic to ferromagnetic transition, in good agreement with our conclusion based on the Arrott plots.

Several RT_2-based compounds with $MgCu_2$-type structures have been found recently to exhibit a large magnetocaloric effect. For example, the change in magnetic entropy corresponding to a magnetic field change $\Delta\mu_0H$ starting from a zero field to $B = \mu_0H$, has been obtained to be $-\Delta S_M \approx 30$ J kg^{-1} K^{-1}, 23 J kg^{-1} K^{-1}, and 11 J kg^{-1} K^{-1} under the field change 0–5 T for $ErCo_2$ ($T_C = 32$ K), $HoCo_2$ ($T_C = 80$ K), and $DyCo_2$ ($T_C = 140$ K), respectively.[15] We have calculated the magnetocaloric effect in $HoNi_2Mn$ from our magnetization data using the Maxwell thermodynamic relation resulting in the $-\Delta S_M$ values as a function of temperature in Fig. 2(c). The maximum $-\Delta S_M$ values are found to be
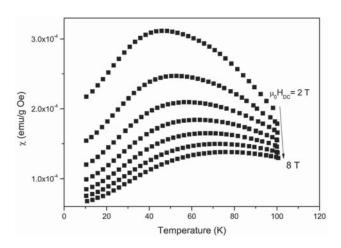
1.5 J kg^{-1} K^{-1}, 3.2 J kg^{-1} K^{-1}, 4.8 J kg^{-1} K^{-1}, 6.0 J kg^{-1} K^{-1}, and 7.4 J kg^{-1} K^{-1} around T_C for field changes of 0–1 T, 0–2 T, 0–3 T, 0–4 T, and 0–5 T, respectively.

Figure 4 shows the neutron diffraction patterns of the $HoNi_2Mn(^{57}Fe)$ sample at $T = 3$ K and 50 K (SPODI diffractometer) below T_C and 300 K (Wombat diffractometer). While direct comparison of the peak intensities is difficult because of the different instruments used, the patterns nonetheless do help to demonstrate the magnetic scattering present in $HoNi_2Mn(^{57}Fe)$ below T_C. In particular, the patterns reveal that below T_C the intensities of the (111) and (220) reflections at 3 K (particularly) and 50 K are increased relative to, say, the nuclear (222) reflection, compared with the behavior of (111) and (220) relative to (222) above T_C at 300 K where $HoNi_2Mn$ is paramagnetic. Rietveld refinement (Fig. 4; small amount of impurity present) indicates that the $8a$ sites are not fully occupied by Ho atoms ($\sim74.1\%$), while Mn atoms occupy $\sim23.8\%$ of the $8a$ sites with about 2.1% of the $8a$ sites empty. By comparison, the $16d$ sites are fully shared by the Ni (74.6%) and Mn (25.4%) atoms. The lattice constant has been derived to be 7.123(3) Å, 7.124(3) Å, and 7.145(3) Å at $T = 3$ K, 50 K, and 300 K, respectively.

Examples of Mössbauer spectra and fits over 5–300 K are shown in Fig. 5. Similar to $TbNi_2Mn$ and $ErNi_2Mn$,[8,9] In the paramagnetic region the spectra indicate features
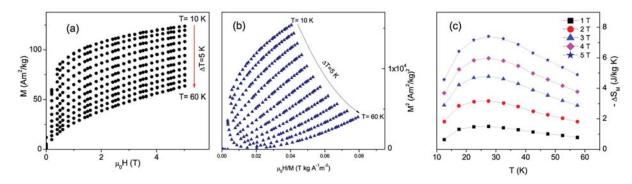

FIG. 2. (Color online) (a) The variation in magnetization of $HoNi_2Mn(^{57}Fe)$ with applied magnetic field $\mu_0H = 0$–5 T at the temperatures indicated. (b) Arrott plot M^2 vs μ_0H/M at the temperatures indicated. (c) Temperature dependence of the isothermal magnetic entropy change $-\Delta S_M(T, H)$.
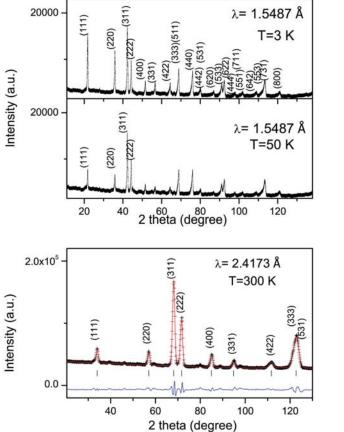
FIG. 4. (Color online) Neutron diffraction patterns for HoNi$_2$Mn sample at $T = 3$ K, 50 K (SPODI, FRM II), and 300 K (Wombat, OPAL).

FIG. 5. (Color online) (a) ^{57}Fe Mössbauer spectra of HoNi$_2$Mn(^{57}Fe) at $T = 5$ K, 70 K, and 300 K. (b) The average isomer shift vs temperature.

consistent with quadrupolar effects, while below T_C the spectra exhibit magnetic hyperfine splitting. We adopted the similar approach as described previously[8]; the spectra above T_C are found to be fitted using two doublets consistent with Mn (and 3d ^{57}Fe atoms) entering both 8a and 16d sites in RNi$_2$Mn compounds. The optimal fits to spectra above T_C have doublets of fractional areas $D_1 \sim 10(1)\%$ and $D_2 \sim 90(2)\%$. Based on the neutron refinement mentioned above, we therefore identify doublet D_1 as representing the behavior of the 8a site with D_2 representing the behavior of the 16d sites.

The spectra below T_C at 5 K show magnetic hyperfine splitting. Similar to TbNi$_2$Mn (^{57}Fe) and ErNi$_2$Mn (^{57}Fe),[8,9] it was found that three sub-sextets are needed to provide optimal fits for the spectra below T_C. The fractional areas of these three sub-sextets are $A_1 \sim 45$ (± 2)% ($B_{hf1} = 16.6$ T), $A_2 \sim 45$ (± 3)% ($B_{hf2} = 12.7$ T), and $A_3 \sim 10$ (± 3)% ($B_{hf2} = 5.7$ T) of overall average $\langle B_{hf} \rangle = 13.7$ T. Based on the transition-metal occupancies of the 16d and 8a sites mentioned above, we conclude that the first two sextets of combined fractional area $\sim 90\%$ correspond to the contribution from ^{57}Fe at 16d sites, with the third sextet representing ^{57}Fe located at the 8a site. Moreover, we also fitted the magnetically split spectra assuming a distribution of hyperfine fields (shown in Fig. 5(a)) with the average field found to be 13.9 T, similar to the value determined for the site model. The Debye temperature of HoNi$_2$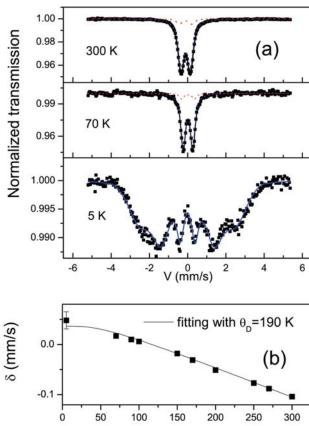Mn(^{57}Fe) has been determined by fitting the temperature dependence of the isomer shift IS(T) in terms of the Debye model (e.g., Ref. 5). The fit (Fig. 5(b)) leads to the Debye temperature $\theta_D = 190 \pm 20$ K.

ACKNOWLEDGMENTS

[1]D. J. Thoma and J. H. Perepezko, J. Alloys Compd. **224**, 330 (1995).
[2]S. B. Gesari *et al.*, J. Phys. Chem. C **114**, 16832 (2010).
[3]J. Nagamatsu *et al.*, Nature **410**, 63 (2001).
[4]A. E. Clark, "Magnetostrictive rare earth-Fe$_2$ compounds, " in *Ferromagnetic Materials*, edited by E. P. Wohlfarth (North-Holland, Amsterdam, 1980), Vol. 1, p. 531.
[5]J. L. Wang *et al.*, Solid State Commun. **121**, 615 (2002); J. L. Wang *et al.*, Phys. Rev. B **73**, 094436 (2006).
[6]D. D. Jackson *et al.*, Phys. Rev. B **75**, 224422 (2007).
[7]N. V. Mushnikov *et al.*, Phys. Rev. B **79**, 184419 (2009).
[8]J. L. Wang *et al.*, J. Phys.: Condens. Matter **23**, 216002 (2011).
[9]J. L. Wang *et al.*, J. Appl. Phys. **109**, 07E304 (2011).
[10]T. H. Jacobs *et al.*, J. Less-Common Met. **157**, L11 (1990).
[11]D. Gignoux *et al.*, Phys. Rev. B **12**, 3878 (1975).
[12]M. R. Ibarra *et al.*, J. Magn. Magn. Mater. **46**, 167 (1984).
[13]K. Inoue *et al.*, J. Phys. Soc. Jpn. **64**, 2175 (1995).
[14]G. Williams, J. Alloys Compd. **326**, 36 (2001).
[15]M. Balli, D. Fruchart, and D. Gignoux, J. Alloys Compd. **509**, 3907 (2011), and references therein.